Cross-orientation masking is speed invariant between ocular pathways but speed dependent within them

Tim S. Meese

School of Life and Health Sciences, Aston University, Birmingham, UK

Daniel H. Baker

School of Life and Health Sciences, Aston University, Birmingham, UK

In human (D. H. Baker, T. S. Meese, & R. J. Summers, 2007b) and in cat (B. Li, M. R. Peterson, J. K. Thompson, T. Duong, & R. D. Freeman, 2005; F. Sengpiel & V. Vorobyov, 2005) there are at least two routes to cross-orientation suppression (XOS): a broadband, non-adaptable, monocular (within-eye) pathway and a more narrowband, adaptable interocular (between the eyes) pathway. We further characterized these two routes psychophysically by measuring the weight of suppression across spatio-temporal frequency for cross-oriented pairs of superimposed flickering Gabor patches. Masking functions were normalized to unmasked detection thresholds and fitted by a two-stage model of contrast gain control (T. S. Meese, M. A. Georgeson, & D. H. Baker, 2006) that was developed to accommodate XOS. The weight of monocular suppression was a power function of the scalar quantity 'speed' (temporal-frequency/spatial-frequency). This weight can be expressed as the ratio of non-oriented magno- and parvo-like mechanisms, permitting a fast-acting, early locus, as befits the urgency for action associated with high retinal speeds. In contrast, dichoptic-masking functions superimposed. Overall, this (i) provides further evidence for dissociation between the two forms of XOS in humans, and (ii) indicates that the monocular and interocular varieties of XOS are space/time scale-dependent and scale-invariant, respectively. This suggests an image-processing role for interocular XOS that is tailored to natural image statistics—very different from that of the scale-dependent (speed-dependent) monocular variety.

Keywords: human vision, psychophysics, contrast gain control, interocular masking, binocular rivalry

Citation: Meese, T. S., & Baker, D. H. (2009). Cross-orientation masking is speed invariant between ocular pathways but speed dependent within them. *Journal of Vision, 9*(5):2, 1–15, http://journalofvision.org/9/5/2/, doi:10.1167/9.5.2.

Introduction

The suppressive effects of grating masks at similar (Phillips & Wilson, 1984), or very different orientations from the target mechanism (Bonds, 1989; DeAngelis, Robson, Ohzawa, & Freeman, 1992; Foley, 1994; Meese & Holmes, 2007; Morrone, Burr, & Maffei, 1982) are often associated with processes in primary visual cortex (Heeger, 1992; Morrone, Burr, & Speed, 1987). However, recent evidence suggests a subcortical contribution to cross-orientation suppression (XOS) in cats (Bonin, Mante, & Carandini, 2005; Freeman, Durand, Kiper, & Carandini, 2002; Li, Thompson, Duong, Peterson, & Freeman, 2006; Priebe & Ferster, 2006; Smith, Bair, & Movshon, 2006) and possibly humans (Baker, Meese, & Summers, 2007b; Cass & Alais, 2006; Meier & Carandini, 2002). Single-cell physiology (Freeman et al., 2002; Li, Peterson, Thompson, Duong, & Freeman, 2005; Sengpiel & Vorobyov, 2005) and psychophysical masking experiments (Baker et al., 2007b; Cass & Alais, 2006; Meese & Hess, 2004) have identified two pathways that mediate XOS. One of these is very broadly tuned for spatial frequency (Bonin et al., 2005) and orientation (Cass & Alais, 2006) and is immune to contrast adaptation (Baker et al., 2007b), consistent with a subcortical locus (Li et al., 2005; Movshon & Lennie, 1979; Sengpiel & Vorobyov, 2005; though see Solomon, Pierce, Dhruv, & Lennie, 2004). The other is less broadly tuned, is desensitized by contrast adaptation, has the same time-course as the detecting mechanism (Baker et al., 2007b), and is presumably cortical (Li et al., 2005, 2006; Sengpiel & Vorobyov, 2005; Sengpiel, Jirmann, Vorobyov, & Eysel, 2006; Webb, Dhruv, Solomon, Tailby, & Lennie, 2005).

The purpose of XOS remains unclear, though several suggestions have been made. One possibility is that it is part of a contrast gain control system whose goal is to normalize cortical contrast-responses to protect population codes against the inherent saturation of visual neurons (Albrecht & Geisler, 1991; Heeger, 1992). A rather different view (Schwartz & Simoncelli, 2001) is that suppressive interactions result in statistical independence of the distributed cortical responses to natural images and that this might influence visual organization. It is also possible that the suppressive interactions are a measurable consequence of a process that sharpens spatial tuning in the cortex (Ringach, Bredfeldt, Shapley, & Hawken, 2002).

In a recent study of binocular masking, Meese and Holmes (2007) found a lawful relation between XOS and

doi: 10.1167/9.5.2 Received August 12, 2008; published May 4, 2009 ISSN 1534-7362

spatiotemporal frequency. The weight of suppression was related to the square-root of the scalar quantity 'speed', given by the ratio of temporal and spatial frequencies: TF/SF. This deviation from scale-invariance casts doubt on a strict interpretation of XOS in terms of natural image statistics. However, it is not known whether this binocular result is inherited from one, the other, or both of the monocular and interocular pathways described above, or even whether it is specific to binocular stimulation.

Here we perform monoptic and dichoptic masking experiments (mask and target in same and different eyes, respectively) to address this issue.

Methods

Equipment

A ViSaGe (Cambridge Research Systems, Kent, UK) running in pseudo-14bit mode was used for one observer (DHB), and a VSG2/4 (CRS) running in pseudo-15bit mode was used for the other two observers. A 120 Hz Clinton Monoray monitor (CRS) with a maximum luminance of 220 cd/m^2 and mirror stereoscope arrangement (previously described in Baker et al., 2007b) was the same for all observers. Neutral density filters were used to reduce the maximum luminance at the eye to 28 cd/m^2.

Stimuli

A carefully calibrated mirror stereoscope allowed mask and target stimuli to be presented to the same (monoptic) or different (dichoptic) eyes. Stimuli were orthogonal patches of sinusoidal grating (target horizontal, mask vertical), windowed by a Gaussian spatial envelope (i.e. Gabor functions). Spatial frequencies were 0.5, 1, 2 and 4 c/deg, and the Gaussian envelope always had a full-width at half-height of 1.65 carrier cycles. Temporal waveforms of 4 and 15 Hz were used. The 4 Hz envelope was a sine wave, multiplied by a raised cosine envelope with a 250 ms central plateau and a total duration of 500 ms. The 15 Hz waveform was a biphasic pulse, with a total duration of 66.7 ms (8 frames at 120 Hz). The four spatial masks and targets and their two temporal envelopes are shown in Figure 1. These stimuli exactly matched a subset of those used in a related study on binocular cross-orientation suppression conducted by Meese and Holmes (2007), where four temporal and five spatial frequencies were used.

Stimulus contrast was controlled using lookup tables, and gamma correction ensured linearity over the full contrast range. Mask and target contrasts were controlled independently using a frame-interleaving technique. This put a theoretical upper contrast limit of 50% on each of the mask and target components. Mask and target contrasts are expressed in decibels (dB), defined as 20 $\log_{10}(C\%)$, where $C\%$ is Michelson contrast in percent, defined as $100(L_{max} - L_{min})/(L_{max} + L_{min})$, where L is luminance.

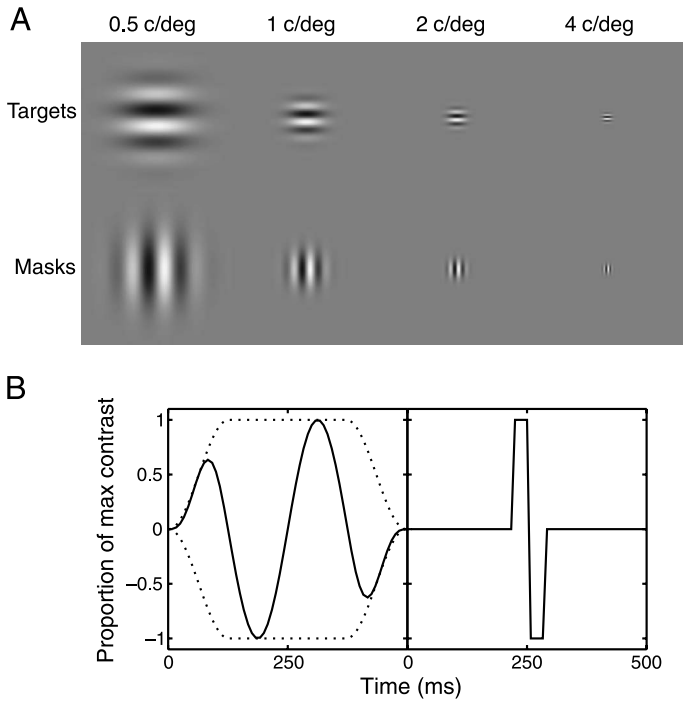

Figure 1. The stimuli used in the experiment. (A) High contrast illustrations of target (top) and mask (bottom) pairs for the four spatial frequency conditions. (B) The two temporal envelopes (dark lines). The gray dotted line in the left panel is the raised cosine part of the 4 Hz envelope. The panel on the right is a 15 Hz biphasic pulse.

Procedure

Observers were seated in a darkened room, with their head in a chin and head-rest, upon which the stereoscope was mounted. All stimuli were presented within 9° circular apertures, offset by ±6° from the center of the screen. The region surrounding this aperture had a nominal luminance of 0 cd/m^2. When viewed through the stereoscope, these apertures were a strong aid to fusion, and appeared as a single central display region. A 'quad' arrangement of four points equidistant from the center of each aperture was used to aid fixation. The points were placed 3 cycles of the carrier grating away from the center, so their positions varied with the spatial frequency of the stimulus (Meese & Holmes, 2007). We avoided using a central fixation point so as not to confound the suppression that we wished to measure here with the suppression that can arise from that type of fixation point (Meese & Hess, 2007; Summers & Meese, 2007).

A temporal two-interval forced-choice (2IFC) paradigm was used, where the mask was presented in both intervals, but the target was presented in only one, selected at random. Observers used mouse buttons to indicate which interval they believed contained the target, and were given auditory feedback regarding their accuracy. The duration between the offset of the first interval and the onset of the second interval was 400 ms.

Stimuli were blocked by mask contrast (0%, 3, 15, 20, 25, 30 and 33 dB), and spatio-temporal condition. Subjects completed one repetition of all mask contrasts and temporal frequencies (in a random order) at a given spatial frequency, before moving on to the next spatial frequency. Within each experimental session, four interleaved staircases (using a 3-up, 1-down configuration; Wetherill & Levitt, 1965) tracked performance, one each for monoptic and dichoptic conditions where targets were in the left or right eye. Each staircase began with a large step-size of 12 dB. This was reduced to 3 dB after the first reversal, where it remained for the rest of the session. Each staircase terminated after 12 reversals of direction (approximately 48 trials). A single session took about 4 minutes (15 Hz) or 8 minutes (4 Hz) to complete.

The entire experiment was repeated three times by each observer, and the results were pooled across repetition and target eye (i.e. six sessions in total), before using probit analysis (Finney, 1971) to estimate a threshold (75% correct).

Observers

Three observers took part in the experiment. DHB is one of the authors (male, aged 24) and WS and KP were undergraduate optometry students (both male, aged 20). The undergraduates were psychophysically naive, and participated as part of their course requirements. All three observers were emmetropic and had no anomalies of binocular vision.

Results

Cross-orientation masking

Cross-orientation masking-functions are shown in Figure 2. For each observer, the figure panels are arranged such that the fastest speed condition (lowest SF, highest TF; 30 cycles per sec) is in the lower left-hand corner, and the slowest speed condition (highest SF, lowest TF; 1 cycle per sec) is in the upper right-hand corner (c.f. Meese & Holmes, 2007). Within each panel, the horizontal dotted line indicates the detection threshold for the baseline condition (0% mask contrast). This is lowest at spatial frequencies of 0.5 and 1 c/deg, and increases with spatial and temporal frequency.

Regardless of whether the mask and target were presented to the same or different eyes (different symbols), there was a general trend for contrast detection thresholds to increase with mask contrast. In addition to this, a small amount of facilitation was also found in some of the monoptic conditions. We will return to this below.

Monoptic masking (blue circles) was strongest at high speeds (lower left corners), but much weaker at lower speeds (upper right corners). This is very similar to the pattern of results found by Meese and Holmes (2007) for binocular targets and masks. Dichoptic masking (green diamonds) appears less dependent on speed than monoptic masking (blue circles) and in most cases was more potent, though in a few cases, this pattern was clearly reversed (e.g. 0.5 c/deg, 15 Hz, DHB and WS).

For observer KP, the baseline at 4 c/deg, 15 Hz (bottom right-hand corner), was particularly high (19%). This meant that the thresholds (75% correct) were often outside the displayable contrast-range of the equipment (a maximum of 50% owing to the frame interleaving) and were extrapolated by the probit procedure. To avoid contamination from unreliable estimates, the results for this condition were omitted from further analyses.

Normalization

Although masking generally appears weaker towards the upper right-hand corners in Figure 2, this might be related to the lower sensitivity (higher baselines) in those regions. This is assessed in Figure 3 where data are normalized to detection threshold on both axes (i.e. mask and target contrasts are expressed in threshold units of the target). For each observer, the different panels show results for the monoptic (top) and dichoptic (bottom) arrangements, for each of the eight spatiotemporal conditions (seven for KP).

In the monoptic condition, the masking-functions fan out, similar to that reported for the binocular case by Meese and Holmes (2007). This shows that the strength (weight) of monoptic cross-orientation masking is affected by the spatial and/or temporal characteristics of the stimulus. In contrast, the dichoptic results appear to collapse onto a single masking-function. This is particularly striking for DHB and KP. For WS there is some spread in the dichoptic masking functions, though it is clearly less extensive than for his corresponding monoptic results (compare top and bottom panels in the middle column of Figure 3). These masking functions suggest that the weight of superimposed dichoptic masking is unaffected by the spatial and temporal frequency of the stimuli (once overall sensitivity is taken into account). This implies that dichoptic cross-orientation masking is scale-invariant in space and time.

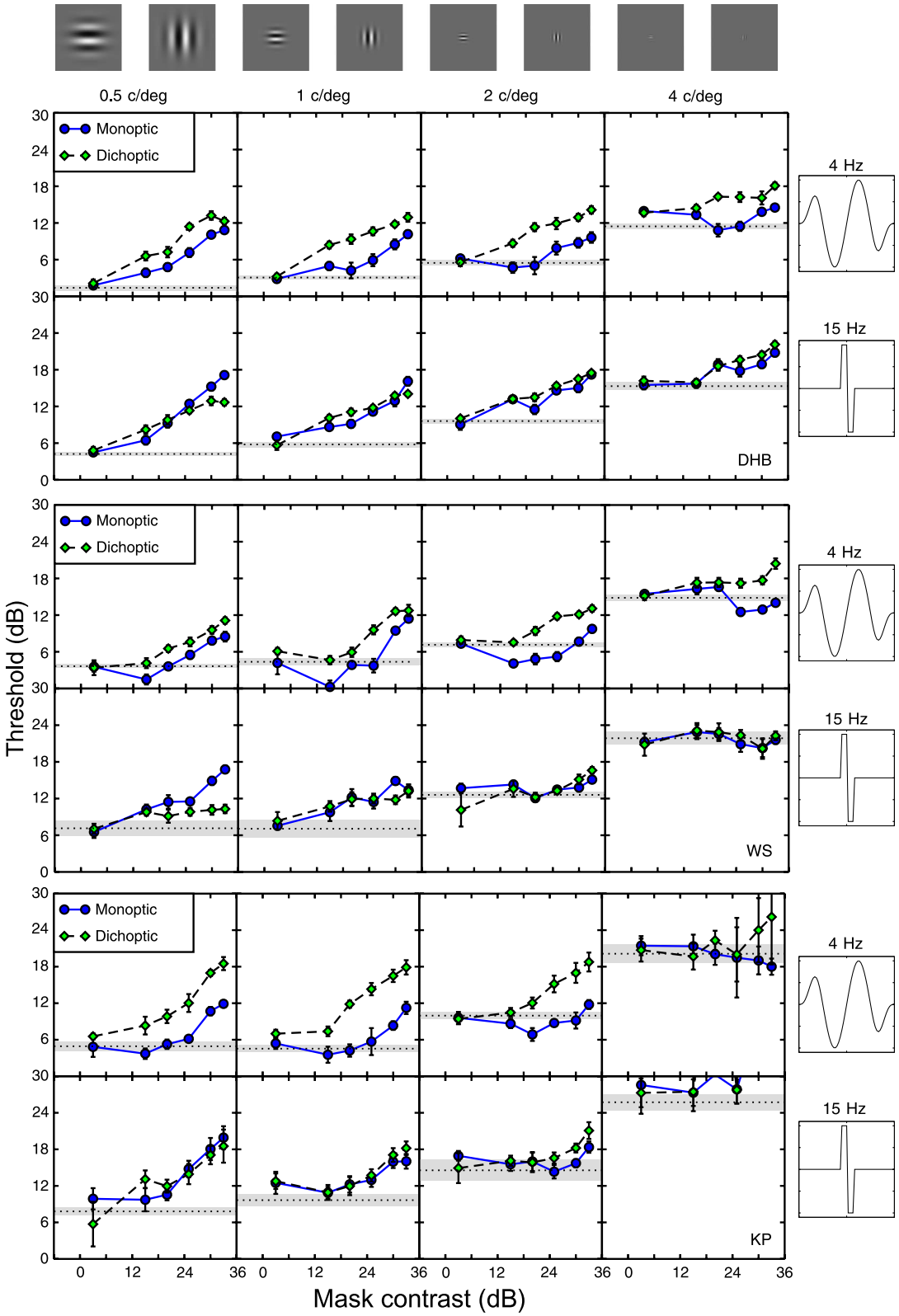

Figure 2. Monoptic (blue circles, solid lines) and dichoptic (green diamonds, dashed lines) cross-orientation masking for eight different spatiotemporal frequencies. The three different groups of plots are for three different observers. Within each group, spatial frequency (SF) increases by panel from left to right (see target and mask icons above top row). Temporal frequency (TF) is 4 Hz in the upper rows, and 15 Hz in the lower rows (see right hand icons). The fastest speed (TF/SF) is in the bottom left hand corners, and the slowest speed is in the top right hand corners. Horizontal dotted lines are baseline detection thresholds (mask contrast of 0%) and gray regions and error bars show ±1 *SE* of the probit fit.

We consider each of these main results in more detail in the modeling section below.

Facilitation

Figure 3 also emphasizes the evidence for cross-orientation facilitation in the monoptic condition (Figure 3, top) for two of the three observers (WS and KP) and its near absence in the dichoptic condition (Figure 3, bottom). Facilitation for superimposed binocular cross-oriented masks was found by Meese and Holmes (2007), Meese, Holmes, and Challinor (2007), and Meese, Summers, Holmes, and Wallis (2007). Using monoptic and dichoptic cross-oriented masks, Baker et al. (2007b) found a similar result to that here. Huang, Hess, and Dakin (2006) also found a similar result for monoptic and dichoptic co-oriented flanker masks, as did Meese and Hess (2004) for monoptic and dichoptic annular masks.

The monoptic facilitation here has a very different character from the within-channel facilitation found with pedestal masks, where the mask has the same spatial properties as the target (Legge & Foley, 1980). In that case, facilitation from a pedestal is typically maximal when the pedestal contrast is close to its own detection threshold. However, the greatest facilitation here arises at much higher relative contrasts, around 12 dB (four times) higher than detection threshold, and is therefore not easily attributed to subthreshold summation.

Another explanation for facilitation is that the mask reduces the observer's uncertainty about which target mechanisms to monitor (Pelli, 1985). However, a reduction of uncertainty should also reduce the slope of the psychometric function (Pelli, 1985; Petrov, Verghese, & McKee, 2006; Tyler & Chen, 2000) and there is very little evidence for this here (Figure 4). Although we do not yet have a detailed understanding of the facilitation here, we have implemented it in our model (next section) by allowing the mask to modulate the target contrast term (Chen & Tyler, 2001; Meese & Holmes, 2007; Meese, Holmes, et al., 2007; Meese, Summers, et al., 2007; Yu, Klein, & Levi, 2003).

Modeling

To fit our experimental results we followed Baker et al. (2007b) and developed the two-stage model of contrast gain control (Meese, Georgeson, & Baker, 2006) for the situation here. This model involves divisive interocular suppression within and between ocular channels, both of which are placed before binocular summation (Baker et al., 2007b). The observer's internal response at the monoptic stage (stage 1) to a target or orthogonal mask (*cmpnt*) in the left eye is given by:

$$stage1L(cmpnt) = \frac{C_L^m}{S + C_L + C_R + \omega_M X_L + \omega_D X_R}, \quad (1)$$

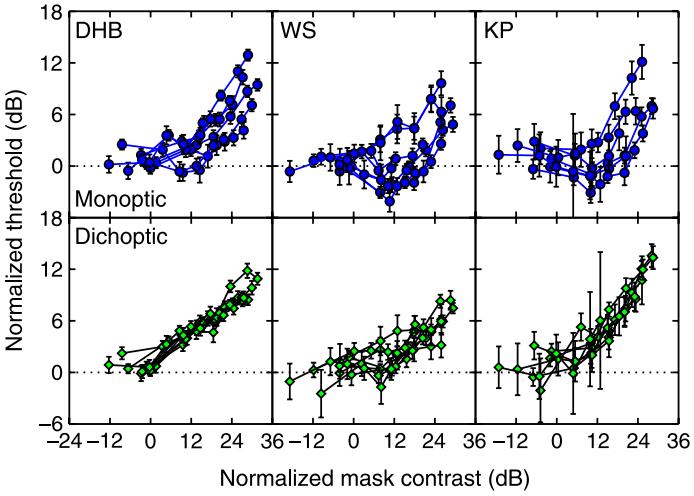

Figure 3. Normalized cross-orientation masking-functions. Upper and lower panels are for monoptic and dichoptic results respectively. Each spatiotemporal masking-function (eight per panel, seven for KP) has been normalized to detection threshold along both axes (sensitivity to vertical and horizontal orientations is assumed to be the same). Data points below the dashed horizontal line indicate facilitation, and those above it indicate masking. Note that mask contrasts below 0 dB are sub-threshold. Error bars show ±1 *SE* of the probit fit.

where C_L and C_R are the component contrasts (target or mask) that drive the stage, and X_L and X_R are the orthogonal contrasts (mask or target) for the two eyes. Note that for the experiments here one of the C terms and one of the X terms was always zero. The parameters S, m, ω_M and ω_D are the saturation constant of the gain control, the excitatory exponent, and the weights of the two cross-oriented terms, respectively. The main aim of the modeling was to establish the values of the two weight parameters for each spatiotemporal condition.

The binocular summation stage is given by:

$$binsum(cmpnt) = stage1L(cmpnt) + stage1R(cmpnt), \quad (2)$$

where the second term on the right hand side is the right eye equivalent of Equation 1. The output stage of the model in response to the target (i.e. the decision variable) is given by:

$$resp(target) = \frac{(1 + \alpha[binsum(mask)])binsum(target)^p}{Z + binsum(target)^q}, \quad (3)$$

where Z is the saturation constant of this stage, p and q are excitatory and suppressive response exponents, and α is a parameter that controls the weight of facilitation (Meese & Holmes, 2007; Meese, Holmes, et al., 2007; Meese,

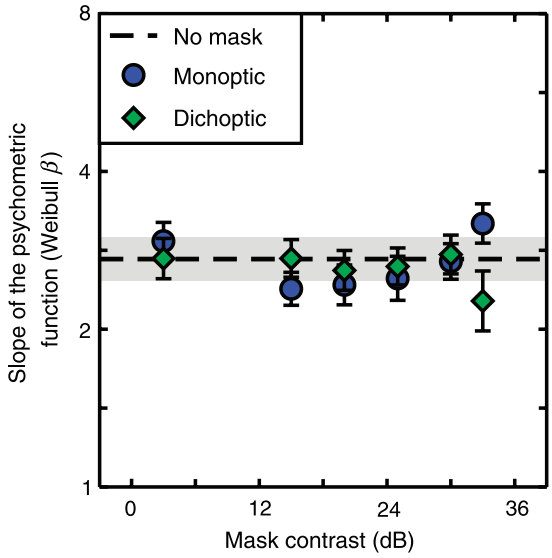

Figure 4. Slopes of the psychometric functions averaged (geometric means) across observer and spatiotemporal frequency for each of the two ocular conditions (different symbols) as functions of mask contrast. The slope is the β parameter from the Weibull function, converted using the approximation: $\beta = 10.3/\sigma$, where σ is the spread parameter (in dB) derived by probit analysis for log contrast units. Each slope estimate was based on data gathered contemporaneously by a pair of staircases, one for each eye. To lessen the impact of outliers, β was capped at $\beta = 10$. This happened in 29 out of 932 estimates (3.1%). The horizontal dashed line is the baseline measure when the mask contrast was 0%. Error bars and gray region show ±1 *SE* of the various estimates.

Summers, et al., 2007). To solve the model equations, the target contrast was adjusted until $resp(target) = k$, where k is a free parameter and is proportional to the standard deviation of late, additive, performance-limiting noise. Thus, the model contains a total of nine free parameters. However, for the experiments here, precise values of several of these parameters were not important and we were able to round five of them from previous results (Meese et al., 2006), giving: $m = 1.3$, $p = 8$, $q = 6.5$, $S = 1$ and $k = 0.2$. The saturation constant Z was then adjusted ($Z = 0.0085$) so that the model produced the correct intercept (0 dB) on the normalized axes.

Values of the remaining three free parameters (α, ω_M and ω_D) were determined using a simplex algorithm to optimize the fits of the model to the results. The model was fitted simultaneously to the monoptic and dichoptic results from all eight spatiotemporal conditions. Following Meese and Holmes (2007), α was yoked across conditions (for each observer, a single value was fitted for the entire experiment), whereas the two suppressive weight parameters were allowed to vary across spatiotemporal conditions. Thus, for observers DHB and WS, we fitted 16 masking functions (to the normalized results) with 17 free parameters. For KP we fitted 14 functions with 15 free parameters. The fits are shown in Figure 5 and the free parameters and figures of merit are shown in Table 1.

Model results

Overall, the fitting provided a good account of the data; the root mean square error of the fit (RMSe) was less than 1.3 dB for each observer (see Table 1 and Figure 5). Note that even though the facilitation stage is binocular (Equation 3), it is able to capture the different monoptic and dichoptic facilitatory effects (Figure 3) with a single value of α for each observer (Table 1). This is because the facilitatory influence of α is apparent in the masking functions only when the masking effect is weak (Meese & Holmes, 2007). For the study here, the masking is weakest for the slow speeds and monoptic masking, and this is where facilitation is seen in the masking functions (Figure 5).

Suppressive weight analysis

We analyzed the fitted weights in Table 1 to see if they showed relations with any of the stimulus parameters. We found that the dichoptic weight (ω_D) was independent of temporal frequency, spatial frequency and the ratio of these two parameters (TF/SF) (see Table 2, and green diamonds and dashed lines in Figure 6). There was some evidence for relations between the monoptic weights (ω_M) and each of temporal frequency and spatial frequency (Table 2). However, the greatest variance (97% for the average) was accounted for by the relation between ω_M and speed (TF/SF) (Table 2).

Figure 6 illustrates the clear distinction between the two forms of masking on double-log axes. The monoptic weights (blue circles) increase with speed, proportional to $(TF/SF)^{0.78}$. This is somewhat steeper than the regression slope of 0.51 found by Meese and Holmes (2007) for binocular XOS, using a simpler version of the model and different observers. But we caution against attributing too much significance to the precise value of the monoptic regression slope here (Figure 6; blue circles). We found that we were able to achieve almost equally good fits to the masking functions in Figure 5 by using much lower values of p and q. For example, with $p = 3.33$ and $q = 2$ (and Z adjusted accordingly), we found an average regression slope (c.f. Figure 6) of 0.51, the same as that in the Meese & Holmes study.[1] However, as several of the (nine) model parameters (Equations 1, 2, and 3) were poorly constrained by the present data set, we preferred the simplicity (and transparency) of the main method used here, where the parameters were set according to those determined from previous data sets. Nonetheless, it is possible that future work might converge on a (slightly) different regression slope from that reported here[2].

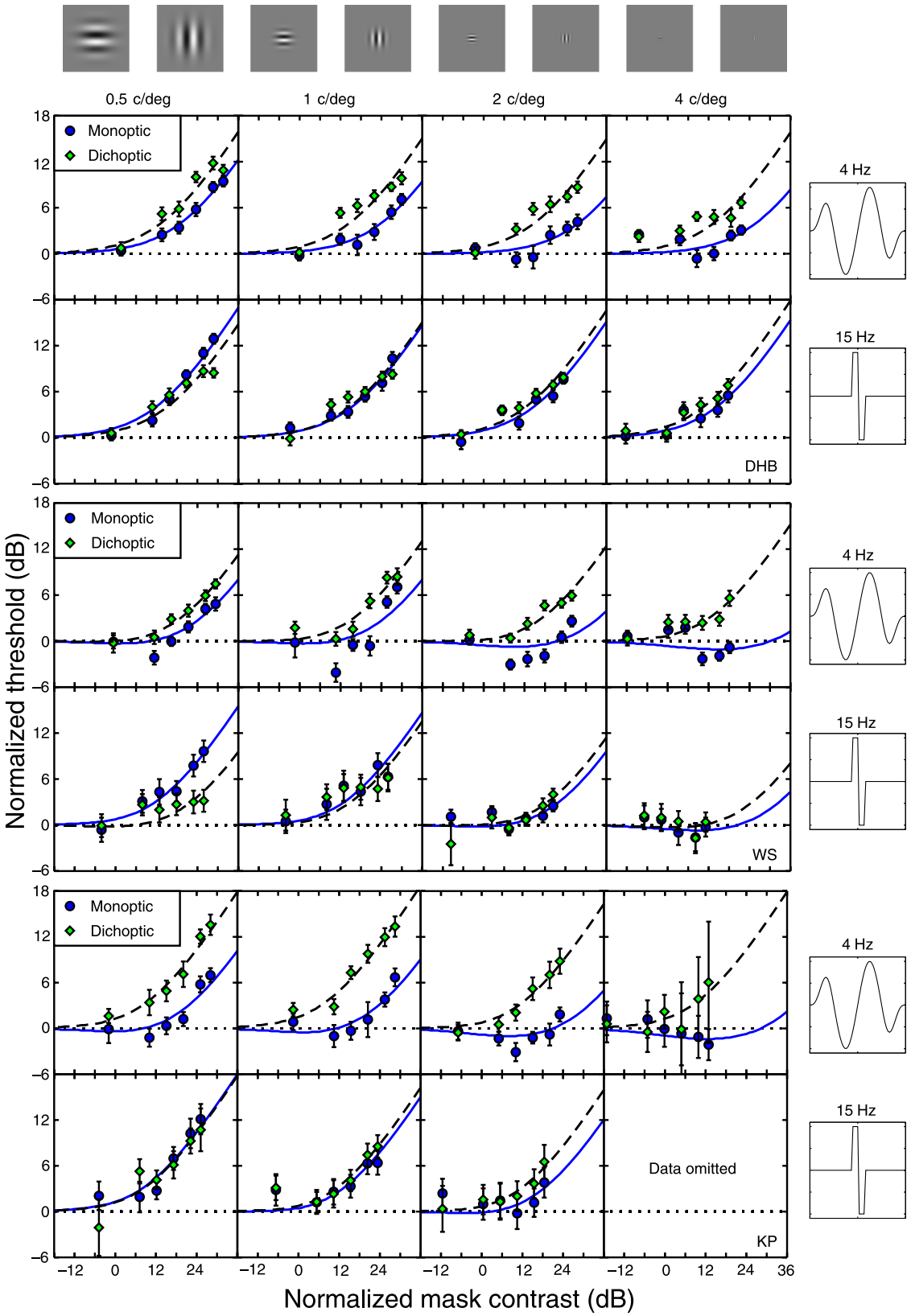

Figure 5. Model fits (curves) to masking functions normalized to baseline sensitivity (mask contrast = 0%). Layout and other details are as for Figure 2. The results for subject KP at 4 c/deg, 15 Hz were omitted for reasons described in the text. For each observer the overall average RMS error of the fits was <1.3 dB. Model parameters are reported in Table 1. Error bars show ±1 *SE* of the probit fit.

Condition		Parameter	DHB	WS	KP
SF (c/deg)	TF (Hz)	α	0	0.70	1.20
0.5	4	ω_M	0.118	0.076	0.126
0.5	15	ω_M	0.274	0.292	0.477
1	4	ω_M	0.067	0.076	0.103
1	15	ω_M	0.183	0.254	0.292
2	4	ω_M	0.043	0.031	0.045
2	15	ω_M	0.200	0.103	0.176
4	4	ω_M	0.054	0.014	0.022
4	15	ω_M	0.206	0.034	–
0.5	4	ω_D	0.228	0.140	0.471
0.5	15	ω_D	0.187	0.102	0.461
1	4	ω_D	0.200	0.193	0.545
1	15	ω_D	0.197	0.209	0.359
2	4	ω_D	0.192	0.171	0.362
2	15	ω_D	0.257	0.144	0.342
4	4	ω_D	0.224	0.278	0.471
4	15	ω_D	0.321	0.077	–
RMSe (dB)			1.008	1.267	1.100

Table 1. Parameter values and figures of merit (RMS error) for the model-fits to the results for each of three observers (Figure 5).

In contrast to the monoptic weights, Figure 6 shows the absence of a speed dependency for the dichoptic weights (green diamonds; the average regression slope was −0.06). This confirms our initial impression (Figure 3) that dichoptic cross-orientation masking is spatiotemporally scale invariant.

Discussion

Cross-orientation masking was measured over a wide range of spatiotemporal frequencies (almost a five-octave range of speeds), for monoptic and dichoptic ocular configurations of mask and target. When mask and target were presented to the same eye, the weight of masking was a power function of stimulus speed (a log-log slope of 0.78). Small levels of facilitation were also found. When mask and target were presented to different eyes, there was no facilitation, and masking was equally potent at all spatiotemporal frequencies (on normalized axes). In sum, there is a distinct lawful dependency on spatiotemporal frequency for the monocular suppressive pathway, but a clear independence of this factor in the interocular pathway (this is the key result, summarized in Figure 6).

Two routes to cross-orientation suppression

An important pre-cursor to the study here was that of Baker et al. (2007b). They measured contrast detection thresholds for patches of gratings in the presence of cross-oriented grating masks presented to either the same or the other eye from the target. They considered the four different logical arrangements of monocular and interocular XOS relative to excitatory binocular summation. If XOS were placed entirely after full binocular convergence, then monoptic and dichoptic masking would be identical. This is not what they found. If just one of the pathways asserted its influence before binocular summation, then masking for the condition specific to that pathway (monoptic or dichoptic) would always be greater than or equal to that for the other condition, owing to the double impact that would arise for that condition (pre- and post-binocular summation). However, this is not what they found either. Instead, they found a complex set of results where the stronger form of XOS (monoptic or dichoptic) depended on interactions across spatial configuration of the mask, stimulus duration and observer. The only model arrangement with sufficient flexibility to accommodate these results was one where both monocular and interocular pathways for XOS asserted their influences before binocular summation. The study here confirms this general observation; in most of Figure 3, dichoptic masking is more potent than monoptic masking, but there are examples where this is the other way around. This is also evident in the weights plotted in Figure 6 where they cross over, particularly for WS.

Speed-dependency for monoptic and binocular masking

The close similarity between the monoptic results here and the binocular results of Meese and Holmes (2007) is striking, and suggests common underlying processes. As noted previously, monoptic- and binocular-masking have similar properties, as one might expect from the simple observation that (with the exception of stereo-depth), the world looks very similar when viewed with either one eye or two (Baker, Meese, & Georgeson, 2007a; Meese et al., 2006). But what might be the basis for the speed dependency in each of these ocular arrangements?

Could monoptic masking arise from response compression in the LGN?

Recent single-cell physiology suggests that monoptic cross-orientation masking occurs because of the compressive response nonlinearity in the LGN (Li et al., 2006; Priebe & Ferster, 2006). As isotropic visual neurons in the LGN would respond to both our mask and target components, this could be the origin of the monoptic masking here. Furthermore, as *m*-cells are responsive to low spatial and high temporal frequencies, fast *m*-type stimuli might produce the strong masking we found because of their distinct contrast-response nonlinearity

	SF (r^2)	TF (r^2)	TF/SF (r^2)
Monoptic			
DHB	0.093	0.812**	0.666*
WS	0.581*	0.353	0.932**
KP	0.580*	0.641*	0.980**
Average	0.436	0.553*	0.970**
Dichoptic			
DHB	0.347	0.105	0.057
WS	0.011	0.308	0.193
KP	0.091	0.274	0.014
Average	0.013	0.396	0.104

Table 2. Regression analysis (linear regression on double-log coordinates) for monoptic and dichoptic model weights against spatial frequency (SF), temporal frequency (TF) and speed (TF/SF). The average results are regressions for the geometric means of the weights across the three observers. *Note:* Asterisks (* and **) indicate significant ($p \leq 0.05$) and highly significant ($p \leq 0.01$) results, respectively.

(Derrington & Lennie, 1984). Similarly, slow *p*-type stimuli would drive the more linear *p*-cells and therefore produce lower levels of masking. This hypothesis might also go some way towards explaining the weak monoptic facilitation by within-channel summation if there were gentle response acceleration for the initial part of the contrast response of *p*-cells (c.f. Legge & Foley, 1980).

However, there are several problems and challenges for this hypothesis. First, cross-orientation masking has been found for red/green isoluminant patches of grating, indicating that XOS is not purely an *m*-type phenomenon (Medina & Mullen, 2009). Second, both monoptic and dichoptic suppression have been found for (parallel and cross-oriented) annular surrounds using contrast matching (Cai, Zhou, & Chen, 2008; Meese & Hess, 2004), indicating that monoptic masking does not derive purely from excitatory drive. Third, the pooling rule across mask orientations is the same for monoptic and dichoptic masks (Meese, Challinor, & Summers, 2008). This latter result suggests that masking from the two distinct ocular pathways (within and between the eyes) involves similar processes. It is unlikely that this is excitatory drive (as posited by the present hypothesis), since the spatial frequency and orientation differences between Meese et al.'s dichoptic mask and target components (a factor of 3 and 45°, respectively) were too great for their binocular summation within a single detecting mechanism (Holmes & Meese, 2004; Meese et al., 2008). Fourth, the nonlinearity that causes conventional pedestal facilitation (Legge & Foley, 1980) survives cross-orientation masking for the binocular (Foley, 1994; Holmes & Meese, 2004) and monoptic cases (unpublished observations). If this facilitation is to be attributed to an accelerating (cortical) transducer (Chirimuuta & Tolhurst, 2005; Kontsevich & Tyler, 1999; Lu & Dosher, 1999, 2008; Legge, Kersten, & Burgess, 1987; Meese & Summers, 2007), then this poses a challenge to any model that attributes masking to an earlier injection of excitatory drive.

Could monoptic masking be modulated by the ratio of magno and parvo mechanisms?

One viable alternative to the hypothesis above is that monoptic and dichoptic masking each arise from distinct suppressive processes, possibly both involving isotropic inhibitory filters (see Baker & Meese, 2007; Baker et al., 2007b; Meese et al., 2008). But the question remains, how does the speed dependency of suppression originate?

An exact measure of temporal frequency (TF) can be derived from the ratio of an appropriate pair of band-pass and low-pass temporal filters, where the band-pass filter has a higher TF cut and peak sensitivity than the low-pass filter, though the difference need not be great (Hammett, Champion, Morland, & Thompson, 2005; Harris, 1986; Perrone & Thiele, 2002). We will call these TF_m and TF_p respectively. Further, an exact measure of spatial frequency (SF) can be derived from the ratio of a similar pair of spatial frequency filters. We will call these SF_p and SF_m for the high and low SF filters respectively. In fact, for neither TF nor SF is it essential that one of the filters is strictly low-pass; a low frequency tuned band-pass filter will do (see Harris, 1986). In any case, we have TF = TF_m/TF_p and SF = SF_p/SF_m. As the scalar quantity speed is given by TF/SF, it follows that this can be derived from

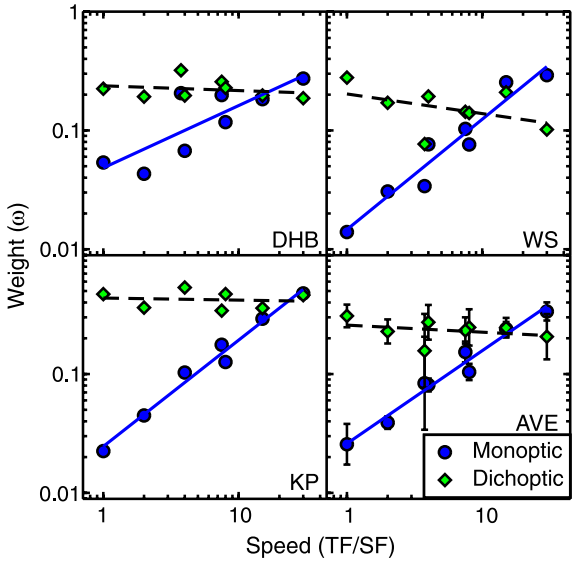

Figure 6. Model weights (from Table 1) for monoptic and dichoptic conditions, plotted against speed (S = TF/SF) for each of three observers and their geometric means (AVE). Straight lines are log-regressions for the function $\omega = AS^{\gamma}$. On average, the monoptic weights increased in proportion to $S^{0.78}$. Exponents for individual observers are: DHB; $\gamma = 0.52$, WS; $\gamma = 0.93$, KP; $\gamma = 0.90$. The dichoptic weights have little or no speed dependence, with exponents close to 0 (DHB; $\gamma = -0.04$, WS; $\gamma = -0.17$, KP; $\gamma = -0.02$; AVE = −0.06).

the ratio of a pair of filters with the spatiotemporal selectivity of TF_mSF_m and TF_pSF_p. While space-time separability is not a property of the entire spatiotemporal contrast sensitivity function (Kelly, 1979), it is much more so for individual cortical cells (Friend & Baker, 1993; Mazer, Vinje, McDermott, Schiller, & Gallant, 2002) and LGN cells (Derrington & Lennie, 1984; Wolfe & Palmer, 1998), and at least some *m*- and *p*-cells in the retina and LGN have the sorts of tuning properties that we require (Derrington & Lennie, 1984; Merigan & Maunsell, 1993). Thus, in principle at least, the scalar quantity, speed, can be derived from the ratio of (linear) filters (*magno*/*parvo*) similar to those found sub-cortex. Furthermore, this computation could be used to modulate the suppressive process that we propose by delivering ω_m (that term would then be raised to an appropriate power, here 0.78), offering a neurophysiological underpinning for our monoptic masking result. The details of this in human remain unclear, though we note that suppressive fields have been identified in the LGN and retina of cat (Bonin et al., 2005; Shapley & Victor, 1978) and monkey (Alitto & Usrey, 2008; Webb et al., 2005). Nonetheless, we cannot rule out the possibility that the monoptic effects that we have measured arise at a slightly later stage such as layer 4 of V1 (Hirsch et al., 2003). However, a stage after binocular summation would not be consistent with the masking results of Baker et al. (2007b), suggesting that speed-dependent XOS for monoptic stimulation asserts its influence no later than V1 (and possibly before).

The proposal here represents an application of a speed computation at a much earlier stage in visual processing than the cortical MT-stage with which it is usually associated. However, those schemes are concerned with the vector quantity, velocity (speed and direction) (Perrone, 2005; Perrone & Krauzlis, 2008; Perrone & Thiele, 2002) and so it is not surprising that they are placed beyond the primitive scalar speed computation that we have described.

Although we have emphasized an early (possibly sub-cortical) locus for the suppressive monocular pathway, we do not wish to imply that there is no cortical route for monoptic masking. Indeed, the evidence for an orientation-tuned component in monoptic masking (Phillips & Wilson, 1984) suggests that there is also a suppressive component with cortical origins, since the cortex is the first stage at which marked orientation tuning arises. Nevertheless, it is likely that the substantial masking found by Phillips and Wilson at low spatial- and high-temporal frequencies owes, at least in part, to an isotropic component of suppression (Meese & Holmes, 2007) and that is plausibly sub-cortical.

What is the purpose of speed-dependent monoptic masking?

We have pointed out that the computation of speed (but not direction) might be available very early in the visual system (pre-binocularity). This might be of benefit since high retinal speeds (excluding those due to head- and eye-movements) indicate a potential need for urgent action (to avoid collision for instance), and so an early warning system would be valuable. But relating this to the specific processes here poses a puzzle. We have found that high stimulus speeds produce the most potent masking, which extends broadly across spatial frequency and orientation (Baker et al., 2007b; Cass & Alais, 2006; Meese, Holmes, et al., 2007), thereby emphasizing the neural representation of the speedy mask. But in doing this, much weaker high-speed signals are completely suppressed from visual awareness. This implies that the visual system attaches greater importance to an uncluttered representation of fast stimuli when the signal (here, the mask) is strong, than to a high sensitivity for other equally fast stimuli but for which the signal is much weaker. Perhaps vision is not an ideal observer for detecting (weak) signals because this strategy conflicts with other demands, as in the case here.

Scale-invariant dichoptic masking and its origins

We have found that after normalizing contrast sensitivity (e.g. Figure 3), the level of dichoptic masking was independent of the spatial and temporal frequency of the target and mask pair (Figure 6). At first sight, the space-time invariance here might seem at odds with our previous report that dichoptic masking increases with stimulus duration (Baker et al., 2007b). However, some care is needed with this. As Baker et al. pointed out, the time-course of dichoptic masking (the way in which the weight of interocular suppression increased from 25 ms to 400 ms) was the same as that of the increase in sensitivity by the contrast detecting mechanism (in the absence of a mask). In other words, the time-dependent dichoptic masking (threshold-elevation) of Baker et al. is invariant with duration (up to 400 ms) if *mask contrast* is normalized to detection threshold, as in our analysis here. Thus, what might appear as contradictory conclusions across the two studies are in fact completely consistent: dichoptic cross-orientation masking depends on the contrast sensitivity to the mask component.

The similarity between the time-course of dichoptic masking and contrast sensitivity (described above) suggests a cortical origin for dichoptic masking (Baker et al., 2007b). This is also consistent with the fact that the cortex is the first stage of substantial interocular interactions. Based on single-cell recordings of amblyopic cats and pharmacological intervention, Sengpiel et al. (2006) also concluded that interocular XOS is a cortical phenomenon.

Finally, we note that other apparently scale invariant effects have also been reported for motion perception (Harris, 1980; Rainville, Scott-Samuel, & Makous, 2002).

Relation to other results

If our general hypothesis is correct then one purpose of cortical suppression might be to provide contrast gain control for stimuli that are not subject to the monocular process, which possibly arises earlier in the visual pathway. This might go some way to explaining a curious result in the temporal-masking study of Cass and Alais (2006). They found that (presumably, binocular) masking was a bimodal masking function for a small 1 Hz target grating (4 c/deg) in the presence of a parallel masking grating (4 c/deg) with variable temporal frequency. The first masking lobe was tuned to the target temporal frequency, whereas the other increased with temporal frequency until reaching a maximum at around 10–15 Hz. This second lobe, but not the first, was also evident using orthogonal masks. We suggest that the first lobe arises from tuned cortical inhibition (either within or between ocular channels), whereas the second lobe is related to the speed-dependent (possibly sub-cortical) suppression here. (Note that speed increases with temporal frequency if spatial frequency is fixed, as it was for Cass & Alais.) Cass and Alais (2006) also considered the possibility that their results might reflect distinct sub-cortical and cortical processes of suppression.

Another intriguing result comes from chromatic masking. On our proposal it seems unlikely that isoluminant gratings would be subject to XOS from the speed-dependent pathway because we suggest that this is driven by the chromaticity-blind *magno* system in the speed computation. (Recall from above, that the weight of suppression in the monocular pathway is a power function of TF/SF, or *magno/parvo,* which would be zero for isoluminant stimuli.) In fact, our preliminary re-analysis of Medina, Meese, and Mullen's (2007) data is consistent with this. For binocular chromatic XOS we found that the weight of suppression was indifferent to speed after normalization (unpublished observations), in stark contrast to the achromatic variety (Meese & Holmes, 2007). A more detailed account of this result awaits future elaboration.

In general, the results here extend our understanding of the dual pathways for cross-orientation suppression. Recent psychophysical experiments have also suggested dual pathways for surround suppression (Cai et al., 2008), and single-cell work indicates the involvement of sub-cortical and cortical components to this form of suppression (Alitto & Usrey, 2008; Webb et al., 2005). Whether these are related to or are different from the two suppressive processes here remains to be seen. One possible way forward would be to establish whether the different types of surround suppression possess the different speed signatures that we have identified (Figure 6).

Finally, the main considerations in the study here involve mask and targets that have the same spatiotemporal frequency as each other. However, in several other studies the spatiotemporal properties of either the mask or the target have been fixed and the orientation, spatial frequency or temporal frequency of the other component has been varied (e.g. Boynton & Foley, 1999; Cass & Alais, 2006; Foley, 1994; Lehky, 1985; Meese, Holmes, et al., 2007; Meese, Summers, et al., 2007; Meier & Carandini, 2002; Phillips & Wilson, 1984; Wilson, McFarlane, & Phillips, 1983). Further work is needed to provide a better understanding of the relation between the results from these types of contrast masking experiments and the study here.

Summary and conclusions

When orthogonal masks and targets are presented to the same eye (monoptic), the strength of masking is a power function of the scalar quantity speed (TF/SF). When the same mask and target are presented to different eyes, the strength of masking is indifferent to speed. We suggest that both processes involve suppressive interactions but through different pathways, both before full binocularity (Baker et al., 2007b). The monoptic effect is consistent with an early sub-cortical stage or possibly pre-binocular stage of V1, whereas the second stage involves binocular interactions and is presumably cortical. The different speed dependencies of the two processes suggest that they contribute to different computational demands. Details of these require further investigation, but it is plausible that the ratio of *magno* and *parvo* units is used to compute monoptic (mask) speed and that this controls suppression in order to emphasize ecologically significant fast-moving stimuli. The interocular cortical stage of suppression is scale invariant in space and time and might be involved in contrast gain control, including that of the color-system. In any case, it is clear that contrast masking will not be fully understood by attempts to attribute a single process to its various manifestations.

Acknowledgments

This work was supported by a grant from the Engineering and Physical Sciences Research Council (GR/S74515/01). We thank Wasim Sarwar and Kishan Patel for their enthusiastic contribution to data collection.

Commercial relationships: none.
Corresponding author: Tim S. Meese.
Email: t.s.meese@aston.ac.uk.
Address: School of Life and Health Sciences, Aston University, Birmingham, B4 7ET, UK.

Footnotes

[1]The illustrative exponent values (p and q) were chosen as follows. In typical model formulations for contrast

discrimination (Legge & Foley, 1980), the log-log slope of the dipper handle is equal to $1 - A$, where A is the difference between the overall exponents on the numerator and denominator of the gain control equation. The effective exponent of the contrast term at the output of stage 1 in our model here is $m - 1$. It follows that the overall exponents on the numerator and denominator at stage 2 are $p(m - 1)$ and $q(m - 1)$ respectively. In our model, $m = 1.3$, and assuming a typical log-log dipper handle of 0.6 (Legge & Foley, 1980), we have $0.6 = 1 - (0.3p - 0.3q)$, which gives us $1.333 = p - q$. We chose an arbitrarily low denominator exponent of $q = 2$, which gives us $p = 3.333$, as we used in the illustration. Note also that as the overall numerator exponent is $p(m - 1)$, then for $m = 1.3$ and $p = 8$, as in our main model analysis, the effective numerator exponent is 2.4, consistent with Legge and Foley (1980).

[2]There is some justification for using lower values of the exponents p and q in the model. With the existing parameters it can be shown that the model here predicts a psychometric function with a Weibull $\beta = 4$. This is slightly steeper than the average $\beta = 2.7$ that we found in the experiment in the absence of a mask (the horizontal dashed line in Figure 4). Reducing the value of p, reduces the model psychometric slope. However, as several other model parameters also influence this function, we chose not to set p according to this constraint. Nevertheless, we emphasize that these model details have little bearing on our main conclusions.

References

Albrecht, D. G., & Geisler, W. S. (1991). Motion selectivity and the contrast response function of simple cells in the visual cortex. *Visual Neuroscience, 7,* 531–546. [PubMed]

Alitto, H. J., & Usrey, W. M. (2008). Origin and dynamics of extraclassical suppression in the lateral geniculate nucleus of the macaque monkey. *Neuron, 57,* 135–146. [PubMed] [Article]

Baker, D. H., & Meese, T. S. (2007). Binocular contrast interactions: Dichoptic masking is not a single process. *Vision Research, 47,* 3096–3107. [PubMed]

Baker, D. H., Meese, T. S., & Georgeson, M. A. (2007a). Binocular interaction: Contrast matching and contrast discrimination are predicted by the same model. *Spatial Vision, 20,* 397–413. [PubMed]

Baker, D. H., Meese, T. S., & Summers, R. J. (2007b). Psychophysical evidence for two routes to suppression before binocular summation of signals in human vision. *Neuroscience, 146,* 435–448. [PubMed]

Bonds, A. B. (1989). Role of inhibition in the specification of orientation selectivity of cells in the cat striate cortex. *Visual Neuroscience, 2,* 41–55. [PubMed]

Bonin, V., Mante, V., & Carandini, M. (2005). The suppressive field of neurons in lateral geniculate nucleus. *Journal of Neuroscience, 25,* 10844–10856. [PubMed] [Article]

Boynton, G. M., & Foley, J. M. (1999). Temporal sensitivity of human luminance pattern mechanisms determined by masking with temporally modulated stimuli. *Vision Research, 39,* 1641–1656. [PubMed]

Cai, Y., Zhou, T., & Chen, L. (2008). Effects of binocular suppression on surround suppression. *Journal of Vision, 8*(9):9, 1–10, http://journalofvision.org/8/9/9/, doi:10.1167/8.9.9. [PubMed] [Article]

Cass, J., & Alais, D. (2006). Evidence for two interacting temporal channels in human visual processing. *Vision Research, 46,* 2859–2868. [PubMed]

Chen, C. C., & Tyler, C. W. (2001). Lateral sensitivity modulation explains the flanker effect in contrast discrimination. *Proceedings of the Royal Society B: Biological Sciences, 268,* 509–516. [PubMed] [Article]

Chirimuuta, M., & Tolhurst, D. J. (2005). Does a Bayesian model of V1 contrast coding offer a neurophysiological account of human contrast discrimination? *Vision Research, 45,* 2943–2959. [PubMed]

DeAngelis, G. C., Robson, J. G., Ohzawa, I., & Freeman, R. D. (1992). Organization of suppression in receptive fields of neurons in cat visual cortex. *Journal of Neurophysiology, 68,* 144–163. [PubMed]

Derrington, A. M., & Lennie, P. (1984). Spatial and temporal contrast sensitivities of neurones in lateral geniculate nucleus of macaque. *The Journal of Physiology, 357,* 219–240. [PubMed] [Article]

Finney, D. J. (1971). *Probit analysis*. Cambridge: Cambridge University Press.

Foley, J. M. (1994). Human luminance pattern-vision mechanisms: Masking experiments require a new model. *Journal of the Optical Society of America A, Optics, Image Science, and Vision, 11,* 1710–1719. [PubMed]

Freeman, T. C., Durand, S., Kiper, D. C., & Carandini, M. (2002). Suppression without inhibition in visual cortex. *Neuron, 35,* 759–771. [PubMed] [Article]

Friend, S. M., & Baker, C. L., Jr. (1993). Spatio-temporal frequency separability in area 18 neurons of the cat. *Vision Research, 33,* 1765–1771. [PubMed]

Hammett, S. T., Champion, R. A., Morland, A. B., & Thompson, P. G. (2005). A ratio model of perceived speed in the human visual system. *Proceedings of the Royal Society B: Biological Sciences, 272,* 2351–2356. [PubMed] [Article]

Harris, M. G. (1980). Velocity specificity of the flicker to pattern sensitivity ratio in human vision. *Vision Research, 20,* 687–691. [PubMed]

Harris, M. G. (1986). The perception of moving stimuli: A model of spatiotemporal coding in human vision. *Vision Research, 26,* 1281–1287. [PubMed]

Heeger, D. J. (1992). Normalization of cell responses in cat striate cortex. *Visual Neuroscience, 9,* 181–197. [PubMed]

Hirsch, J. A., Martinez, L. M., Pillai, C., Alonso, J. M., Wang, Q., & Sommer, F. T. (2003). Functionally distinct inhibitory neurons at the first stage of visual cortical processing. *Nature Neuroscience, 12,* 1300–1308. [PubMed]

Holmes, D. J., & Meese, T. S. (2004). Grating and plaid masks indicate linear summation in a contrast gain pool. *Journal of Vision, 4*(12):7, 1080–1089, http://journalofvision.org/4/12/7/, doi:10.1167/4.12.7. [PubMed] [Article]

Huang, P. C., Hess, R. F., & Dakin, S. C. (2006). Flank facilitation and contour integration: Different sites. *Vision Research, 46,* 3699–3706. [PubMed]

Kelly, D. H. (1979). Motion and vision. II. Stabilized spatio-temporal threshold surface. *Journal of the Optical Society of America, 69,* 1340–1349. [PubMed]

Kontsevich, L. L., & Tyler, C. W. (1999). Nonlinearities of near-threshold contrast transduction. *Vision Research, 39,* 1869–1880. [PubMed]

Legge, G., & Foley, J. (1980). Contrast masking in human vision. *Journal of the Optical Society of America, 70,* 1458–1471. [PubMed]

Legge, G. E., Kersten, D., & Burgess, A. E. (1987). Contrast discrimination in noise. *Journal of the Optical Society of America A, Optics and Image Science, 4,* 391–404. [PubMed]

Lehky, S. R. (1985). Temporal properties of visual channels measured by masking. *Journal of the Optical Society of America A, Optics and Image Science, 2,* 1260–1272. [PubMed]

Li, B., Peterson, M. R., Thompson, J. K., Duong, T., & Freeman, R. D. (2005). Cross-orientation suppression: Monoptic and dichoptic mechanisms are different. *Journal of Neurophysiology, 94,* 1645–1650. [PubMed] [Article]

Li, B., Thompson, J. K., Duong, T., Peterson, M. R., & Freeman, R. D. (2006). Origins of cross-orientation suppression in the visual cortex. *Journal of Neurophysiology, 96,* 1755–1764. [PubMed] [Article]

Lu, Z. L., & Dosher, B. A. (1999). Characterizing human perceptual inefficiencies with equivalent internal noise. *Journal of the Optical Society of America A, Optics, Image Science, and Vision, 16,* 764–778. [PubMed]

Lu, Z. L., & Dosher, B. A. (2008). Characterizing observers using external noise and observer models: Assessing internal representations with external noise. *Psychological Review, 115,* 44–82. [PubMed]

Mazer, J. A., Vinje, W. E., McDermott, J., Schiller, P. H., & Gallant, J. L. (2002). Spatial frequency and orientation tuning dynamics in area V1. *Proceedings of the National Academy of Sciences of the United States of America, 99,* 1645–1650. [PubMed] [Article]

Medina, J., Meese, T., & Mullen, K. (2007). Cross-orientation masking in the red-green isoluminant and luminance systems [Abstract]. *Journal of Vision, 7*(9):257, 257a, http://journalofvision.org/7/9/257/, doi:10.1167/7.9.257.

Medina, J., & Mullen, K. (2009). Cross-orientation masking in human color vision. *Journal of Vision* (in press).

Meese, T. S., Challinor, K. L., & Summers, R. J. (2008). A common contrast pooling rule for suppression within and between the eyes. *Visual Neuroscience, 25,* 585–601. [PubMed]

Meese, T. S., Georgeson, M. A., & Baker, D. H. (2006). Binocular contrast vision at and above threshold. *Journal of Vision, 6*(11):7, 1224–1243, http://journalofvision.org/6/11/7/, doi:10.1167/6.11.7. [PubMed] [Article]

Meese, T. S., & Hess, R. F. (2004). Low spatial frequencies are suppressively masked across spatial scale, orientation, field position, and eye of origin. *Journal of Vision, 4*(10):2, 843–859, http://journalofvision.org/4/10/2/, doi:10.1167/4.10.2. [PubMed] [Article]

Meese, T. S., & Hess, R. F. (2007). Anisotropy for spatial summation of elongated patches of grating: A tale of two tails. *Vision Research, 47,* 1880–1892. [PubMed]

Meese, T. S., & Holmes, D. J. (2007). Spatial and temporal dependencies of cross-orientation suppression. *Proceedings of the Royal Society B: Biological Sciences, 274,* 127–136. [PubMed] [Article]

Meese, T. S., Holmes, D. J., & Challinor, K. L. (2007). Remote facilitation in the Fourier domain. *Vision Research, 47,* 1112–1119. [PubMed]

Meese, T. S., & Summers, R. J. (2007). Area summation in human vision at and above detection threshold.

Proceedings of the Royal Society B: Biological Sciences, 274, 2891–2900. [PubMed] [Article]

Meese, T. S., Summers, R. J., Holmes, D. J., & Wallis, S. A. (2007). Contextual modulation involves suppression and facilitation from the center and the surround. *Journal of Vision, 7*(4):7, 1–21, http://journalofvision.org/7/4/7/, doi:10.1167/7.4.7. [PubMed] [Article]

Meier, L., & Carandini, M. (2002). Masking by fast gratings. *Journal of Vision, 2*(4):2, 293–301, http://journalofvision.org/2/4/2/, doi:10.1167/2.4.2. [PubMed] [Article]

Merigan, W. H., & Maunsell, J. H. (1993). How parallel are the primate visual pathways? *Annual Review of Neuroscience, 16,* 369–402. [PubMed]

Morrone, M. C., Burr, D. C., & Maffei, L. (1982). Functional implications of cross-orientation inhibition of cortical visual cells. I. Neurophysiological evidence. *Proceedings of the Royal Society of London B: Biological Sciences, 216,* 335–354. [PubMed]

Morrone, M. C., Burr, D. C., & Speed, H. D. (1987). Cross-orientation inhibition in cat is GABA mediated. *Experimental Brain Research, 67,* 635–644. [PubMed]

Movshon, J. A., & Lennie, P. (1979). Pattern-selective adaptation in visual cortical-neurons. *Nature, 278,* 850–852. [PubMed]

Pelli, D. G. (1985). Uncertainty explains many aspects of visual contrast detection and discrimination. *Journal of the Optical Society of America A, Optics and Image Science, 2,* 1508–1532. [PubMed]

Perrone, J. A. (2005). Economy of scale: A motion sensor with variable speed tuning. *Journal of Vision, 5*(1):3, 28–33, http://journalofvision.org/5/1/3/, doi:10.1167/5.1.3. [PubMed] [Article]

Perrone, J. A., & Krauzlis, R. J. (2008). Spatial integration by MT pattern neurons: A closer look at pattern-to-component effects and the role of speed tuning. *Journal of Vision, 8*(9):1, 1–14, http://journalofvision.org/8/9/1/, doi:10.1167/8.9.1. [PubMed] [Article]

Perrone, J. A., & Thiele, A. (2002). A model of speed tuning in MT neurons. *Vision Research, 42,* 1035–1051. [PubMed]

Petrov, Y., Verghese, P., & McKee, S. P. (2006). Collinear facilitation is largely uncertainty reduction. *Journal of Vision, 6*(2):8, 170–178, http://journalofvision.org/6/2/8/, doi:10.1167/6.2.8. [PubMed] [Article]

Phillips, G. C., & Wilson, H. R. (1984). Orientation bandwidths of spatial mechanisms measured by masking. *Journal of the Optical Society of America A, Optics and Image Science, 1,* 226–232. [PubMed]

Priebe, N. J., & Ferster, D. (2006). Mechanisms underlying cross-orientation suppression in cat visual cortex. *Nature Neuroscience, 9,* 552–561. [PubMed]

Rainville, S. J., Scott-Samuel, N. E., & Makous, W. L. (2002). The spatial properties of opponent-motion normalization. *Vision Research, 42,* 1727–1738. [PubMed]

Ringach, D. L., Bredfeldt, C. E., Shapley, R. M., & Hawken, M. J. (2002). Suppression of neural responses to nonoptimal stimuli correlates with tuning selectivity in macaque V1. *Journal of Neurophysiology, 87,* 1018–1027. [PubMed] [Article]

Schwartz, O., & Simoncelli, E. P. (2001). Natural signal statistics and sensory gain control. *Nature Neuroscience, 4,* 819–825. [PubMed]

Sengpiel, F., Jirmann, K. U., Vorobyov, V., & Eysel, U. T. (2006). Strabismic suppression is mediated by inhibitory interactions in the primary visual cortex. *Cerebral Cortex, 16,* 1750–1758. [PubMed] [Article]

Sengpiel, F., & Vorobyov, V. (2005). Intracortical origins of interocular suppression in the visual cortex. *Journal of Neuroscience, 25,* 6394–6400. [PubMed] [Article]

Shapley, R. M., & Victor, J. D. (1978). The effect of contrast on the transfer properties of cat retinal ganglion cells. *The Journal of Physiology, 285,* 275–298. [PubMed] [Article]

Smith, M. A., Bair, W., & Movshon, J. A. (2006). Dynamics of suppression in macaque primary visual cortex. *Journal of Neuroscience, 26,* 4826–4834. [PubMed] [Article]

Solomon, S. G., Peirce, J. W., Dhruv, N. T., & Lennie, P. (2004). Profound contrast adaptation early in the visual pathway. *Neuron, 42,* 155–162. [PubMed] [Article]

Summers, R. J., & Meese, T. S. (2007). The influence of fixation points on the contrast detection of patches of grating: AVA Abstract. *Perception, 36,* 1404.

Tyler, C. W., & Chen, C. C. (2000). Signal detection theory in the 2AFC paradigm: Attention, channel uncertainty and probability summation. *Vision Research, 40,* 3121–3144. [PubMed]

Webb, B. S., Dhruv, N. T., Solomon, S. G., Tailby, C., & Lennie, P. (2005). Early and late mechanisms of surround suppression in striate cortex of macaque. *Journal of Neuroscience, 25,* 11666–11675. [PubMed] [Article]

Wetherill, G. B., & Levitt, H. (1965). Sequential estimation of points on a psychometric function. *British Journal of Mathematical and Statistical Psychology, 18,* 1–10. [PubMed]

Wilson, H. R., McFarlane, D. K., & Phillips, G. C. (1983). Spatial-frequency tuning of orientation selective units

estimated by oblique masking. *Vision Research, 23,* 873–882.

Wolfe, J., & Palmer, L. A. (1998). Temporal diversity in the lateral geniculate nucleus of cat. *Visual Neuroscience, 15,* 653–675. [PubMed]

Yu, C., Klein, S. A., & Levi, D. M. (2003). Cross- and iso-oriented surrounds modulate the contrast response function: The effect of surround contrast. *Journal of Vision, 3*(8):1, 527–540, http://journalofvision.org/3/8/1/, doi:10.1167/3.8.1. [PubMed] [Article]